Crystal and Layer Structures of Ferroelectric Oligomer Thin Films

Shuichiro Kuwajima*

NanoMedicine Merger Educational Unit, Department of MicroEngineering, Kyoto University, Sakyo-ku, Kyoto 606-8501 Japan

Satoshi Horie, Toshihisa Horiuchi, Hirofumi Yamada, and Kazumi Matsushige

Department of Electronic Science and Engineering, Kyoto University, Nishikyo-ku, Kyoto 615-8510 Japan

Kenji Ishida

Department of Chemical Science and Engineering, Kobe University, Rokkodai-cho, Nada, Kobe 657-8501, Japan

Received November 25, 2008; Revised Manuscript Received March 16, 2009

ABSTRACT: The crystal structure of ferroelectric vinylidene fluoride (VDF) oligomer [$CF_3(CH_2CF_2)_nI$] (n = 12) thin films has been investigated in detail. Films with molecular orientations parallel and perpendicular to the silicon substrate were prepared by deposition at substrate temperatures of 120 K (low-T_s) and 310 K (high-T_s), respectively. X-ray diffraction revealed a base-centered monoclinic structure with space group *Cm* and lattice parameters $a = 0.488$ nm, $b = 0.865$ nm, and $c = 3.137/\sin\beta$ nm (the monoclinic angle β could not be evaluated). The average density of both films determined from X-ray reflectivity (2.0−2.1 g/cm^3) was lower than that calculated from the lattice parameters (2.42 g/cm^3) due to the surface topology. Small crystal grains are loosely packed in the low-T_s film, while large hexagonal grains increase the surface roughness in the high-T_s film. In both films, furthermore, the even lower density (1.5−1.7 g/cm^3) near the film−substrate interface suggests that the molecules are aligned vertically in this region.

Introduction

Organic ferroelectric materials have attracted constant attention for several decades, ever since the discovery of ferroelectricity in the fluorinated polymers poly vinylidene fluoride (PVDF) and its copolymer with trifluoroethylene (TrFE).[1−7] Practical electronic devices based on ferroelectrics increasingly demand materials that have additional functionality, such as the ability to bend like paper or operate at low applied voltages. Polymeric materials have intrinsically excellent mechanical flexibility due to their complex structures in which crystalline and amorphous regions naturally coexist. However, this structural complexity can make it difficult to quantitatively study the fundamental ferroelectricity that is realized in three-dimensional ordered structures. PVDF has a crystalline polymorph, but the form II (α phase) crystal structure with a nonpolar molecular conformation (*TGTG′*) is predominant under normal conditions.[8,9] In order to realize ferroelectric PVDF it is necessary to stabilize the form I (β phase) crystal structure, which has a planar zigzag (*all-trans*) conformation.[10,11]

With the aim of applying its unique ferroelectric properties to organic thin film devices, VDF oligomer films (a low molecular weight, short chain variant of PVDF) have been intensively investigated by Matsushige et al.[12−16] The short, finite molecular chain length of the oligomer allows the fabrication of thin films with uniform molecular weight distribution using a vacuum evaporation method; this technique is particularly suited to the fabrication of homogeneous, highly crystalline thin films on various substrates.[17] Ishida et al. have recently succeeded in observing high-performance ferroelectric and piezoelectric properties on a flexible polymer substrate, where the magnitude of the polarization was the highest ever measured among organic ferroelectric materials.[18,19] The most important experimental parameter that must be controlled in order to realize the ferroelectric form I phase in thin films is the substrate temperature during deposition, T_s. The molecular orientation is parallel to the substrate when deposition is carried out at $T_s < 150$ K, which yields an electric dipole arrangement parallel to the applied electric field. It has also been reported that VDF oligomer thin films deposited in the nonpolar form II phase exhibit a gradual phase change to the polar form I phase when the substrate is heated at above 380 K.[16] Thus, heating the substrate even during the deposition process may promote formation of the ferroelectric form I structure. These results indicate that the ferroelectric form I structure of the VDF oligomer can be prepared under at least two different sets of experimental conditions.

Despite advances in the fabrication of ferroelectric VDF oligomer films, precise details of the crystal structure, including the unit cell parameters, crystal system and space group, have not been investigated because single crystals of the ferroelectric phase are difficult to prepare. Tashiro and Hanesaka successfully determined the crystal structure of the nonpolar, form II bulk oligomer $CF(CF_3)_2(CH_2CF_2)_nI$. The unit cell parameters were different to those of PVDF, although the local molecular packing structure was essentially the same.[20] Knowledge of the unit cell structure and the corresponding crystallographic symmetry are obviously essential in order to understand the ferroelectric properties. The crystal structure of the thin film oligomer may be different to that of the bulk oligomer due to the strong interaction with the substrate during growth. Therefore, a precise understanding of the layer structure, particularly at the interface between the film and the substrate, is also important. In this study we fabricate highly crystalline and molecularly oriented VDF oligomer thin films with the ferroelectric form I structure. Furthermore, we evaluate the unit cell and layer structures using FT-IR, AFM and advanced X-ray scattering measurements. The structural details that we uncover will not only provide further insight into the fundamental ferroelectric properties of these uniform, finite-length molecular chains but will also bring

* Corresponding author: kuwajima@me.kyoto-u.ac.jp.

10.1021/ma802639r CCC: $40.75
Published on Web 04/09/2009

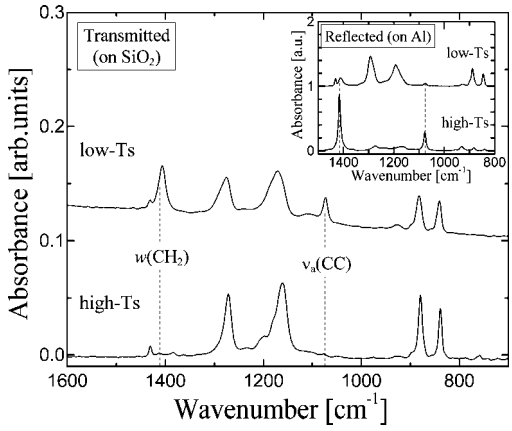

Figure 1. Transmitted FT-IR spectra for VDF oligomer thin films deposited on silicon substrates under low-temperature (upper) and high-temperature (lower) conditions. The C−C antisymmetric stretching mode [ν_a(CC)] at 1070 cm^{-1} and the CH_2 wagging mode [$w(CH_2)$] at 1410 cm^{-1}, parallel to the molecular axis, are marked by dashed lines. In the inset, reflected spectra of both films on aluminum substrates are also described.

practical applications using organic ferroelectric materials a step closer.

Experimental Section

The VDF oligomer [$CF_3(CH_2CF_2)_nI$] ($n = 12$) was synthesized by Daikin Kogyo Co. Ltd. Thin films of the oligomer were fabricated by vacuum evaporation (~10^{-6} Pa) on a silicon wafer with a naturally oxidized surface. In order to obtain the ferroelectric *all-trans* conformation, the thin films were deposited under two sets of experimental conditions. The substrate temperature T_s was fixed at either 120 or 310 K during the deposition. After deposition the substrate temperature was either increased or decreased to room temperature. The deposition rate was 1 nm/min and the nominal thickness of the films was approximately 150 nm, as monitored by a quartz oscillator. The thin films deposited at 120 and 310 K are referred to below as low-T_s and high-T_s films, respectively.

X-ray scattering measurements were carried out at room temperature in air using a high-resolution diffractometer (RIGAKU ATX-G). The Cu Kα_1 radiation ($\lambda = 0.154$ nm) was monochromatized using a germanium channel-cut double crystal. The specular X-ray reflectivity was measured by a typical $2\theta-\omega$ scan ranging 0−2 deg; the beam size was 0.05 (h) × 2 (v) mm^2 in the vertical setting of the substrate. The layer structure, average density, thickness and interface roughness of the films were calculated using the software 'GXRR' for fitting X-ray reflectivity profiles. The molecular conformation was studied using Fourier transform infrared (FT-IR) spectroscopy (JASCO FT/IR-660 plus) in both reflection and transmission modes; the polarized infrared beams show strong interaction between molecular vibrations parallel (transmission) and perpendicular (reflection) to the substrate, respectively. It is noted that an aluminum thin film (thickness ~50 nm) was deposited between the substrate and the oligomer film in the reflection mode. The FT-IR measurements were executed under low vacuum conditions (~100 Pa). Dynamic-mode atomic force microscopy (AFM) measurements were performed to observe the surface morphology (JEOL JSPM-5200).

Results and Discussion

Figure 1 shows the transmitted FT-IR spectra of the low-T_s and high-T_s films. In both spectra, a series of absorption peaks characteristic of the *all-trans* conformation (form I) with a planar zigzag carbon chain are observed in the range 800−1400 cm^{-1}.[9,14,16] Same as cooling the substrate (123 K) during the deposition process, slightly heating the substrate (310 K) also promotes formation of the *all-trans* conformation; both form I and II structures coexist in films fabricated under normal conditions (~300 K). The C−C antisymmetric stretching mode [ν_a(CC)] at 1070 cm^{-1} and the CH_2 wagging mode [$w(CH_2)$] at 1410 cm^{-1}, which are the vibrations parallel to the molecular axis, disappeared in the spectrum of the high-T_s film. In contrary, the peaks became more intense in the low-T_s film. It is therefore suggested that the oligomer molecules in the ferroelectric form I structure of both films have a different uniaxial orientation, aligning perpendicular (high-T_s) and lying parallel (low-T_s) to the substrate. Supporting the transmitted spectra, the reflection mode measurements were carried out for both films on the aluminum substrate, although the molecular conformation and/or orientation might be different in the films with and without aluminum. The spectra are depicted in the inset. In contrast to the transmission measurements, the ν_a(CC) and $w(CH_2)$ vibration modes were intense only in the high-T_s and considerably weak in the low-T_s spectrum, which indirectly supports the uniaxial molecular orientation as mentioned above.

AFM topographic images and line profiles of the low-T_s (left) and high-T_s (right) films on silicon substrates are shown in Figure 2. The scan areas were 1.5 × 1.5 μm^2 (low-T_s) and 5.0 × 5.0 μm^2 (high-T_s). A white line shows the direction and range of the line scan in each case. In contrast to the molecular migration of less than 20 nm observed in the low-T_s image, resulting from deposition on the low-temperature substrate (T_s = 120 K), a remarkable crystal growth phenomenon is observed in the high-T_s image. The hexagonal shape of the crystal grains may be due to the molecular packing structure of PVDF, forming pseudohexagonal *ab* lattice planes. Furthermore, it is also noteworthy that distinct steps with heights corresponding to the oligomer chain length (3−4 nm) appear in the line profile. This indicates that the oligomer molecules are stacked with orientations perpendicular to the substrate during the formation of successive layers, which is entirely consistent with the results of the FT-IR analysis.

The crystal structure in the lateral direction with respect to the substrate was probed by means of in-plane X-ray diffraction measurements (Figure 3). The horizontal axis shows the momentum transfer q ($= 4\pi\sin\theta/\lambda$). The X-ray angle of glazing-incidence was set at 0.22 deg, where the in-plane diffraction intensity was most intense. The diffraction peak patterns were similar in both profiles, which indicates that both high-T_s and low-T_s films mainly adopt the crystal structure of ferroelectric form I. Several X-ray analysis for the form I structure of PVDF have been reported.[1,8,21−24] The crystal structure was precisely determined by Lando et al.[1] and Hasegawa et al.;[8] $a = 0.858$ nm, $b = 0.491$ nm, and c(fiber axis) = 0.256 nm, space group *Cm2m*. Considering the lattice constants and the extinction rule ($h + k = even$), the observed peak pattern of both films show remarkable coincidence with the form I structure of PVDF. As for the high-T_s film, the given indexes were only for *hk*0 reflections, which is consistent with the molecular orientation perpendicular to the substrate. We note that the unit cell setting is different to that of PVDF, with the *a* and *b* axes being reversed. In contrast to the low-T_s profile showing rather weak and broad, the sharper and more intense peaks are due to the highly crystalline layer growth apparent in the AFM topography (Figure 2). As indicated by the dashed circle in Figure 3, the partially overlapping 130 and 200 peaks can be separated by a peak fitting procedure. The lattice spacings d_{130} and d_{200} were calculated as 0.248 and 0.244 nm, respectively. We can assume that the *ab* lattice plane is rectangular since the diffraction pattern corresponds to the orthorhombic crystal system of the form I structure of PVDF. The *a* and *b* lattice parameters can thus be determined as 0.488 and 0.865 nm, respectively.

The standard $2\theta-\omega$ profile (out-of-plane) for the high-T_s film is depicted in the inset of Figure 3. A series of 00*L* peaks was

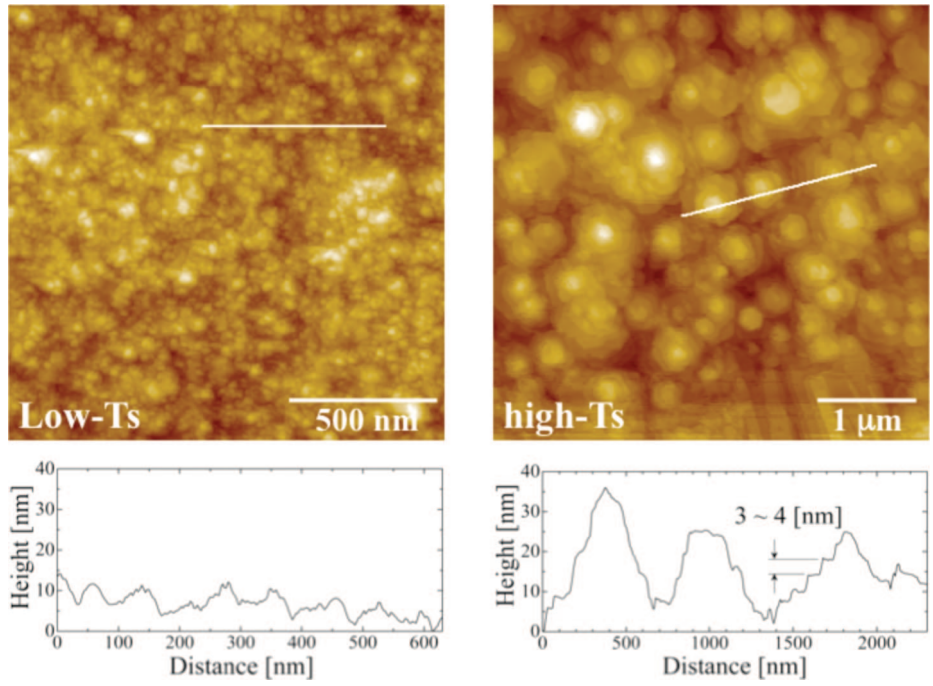

Figure 2. Dynamic mode AFM topographic images and line profiles of the low-T_s (left) and high-T_s (right) films. The scan areas were 1.5 × 1.5 μm^2 (low-T_s) and 5.0 × 5.0 μm^2 (high-T_s). The white lines indicate the direction and range over which the corresponding line scans were taken.

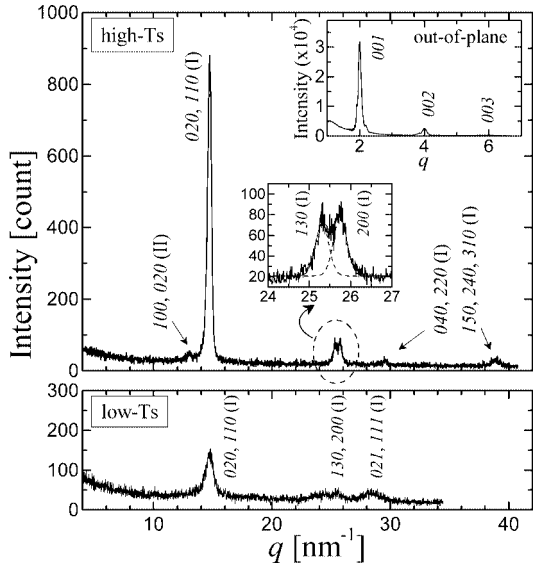

Figure 3. In-plane X-ray diffraction profiles of the high-T_s (upper) and low-T_s (lower) films. The incident X-ray angle was set at 0.22 deg. An expanded view of the resolved 130 and 200 reflections is depicted in the center inset. The standard out-of-plane diffraction profile for the high-T_s film is shown in the upper inset.

observed in the low-q region; the most intense 001 reflection corresponds to a lattice spacing of 3.137 nm. This value is somewhat smaller than the length of a single VDF oligomer molecule ($n = 12$) with the *all-trans* conformation, taking into account the approximate molecular length of 3.3 nm containing the end groups (−I and $-CF_3$) as well as the 12 monomer units $[-CH_2-CF_2-]$ (~0.256 nm). This result indicates that the oligomer molecules are tilted over 10 deg with respect to the substrate normal, and hence, the unit cell has crystallographic symmetry lower than orthorhombic. In order to determine the space group, it is important to establish whether the molecular packing between neighboring oligomer molecules is parallel or antiparallel, since the end groups affect the crystal growth and accordingly the unit cell structure.[20] A parallel arrangement would correspond to a base-centered unit cell, while an antiparallel arrangement would require the presence of a glide plane. Taking these symmetry arguments into consideration, we can conclude that the C-centered (base-centered) monoclinic system with space group *Cm* is adopted, where $a = 0.488$ nm, $b = 0.865$ nm, and $c = 3.137/\sin\beta$ nm. Unfortunately, the angle β could not be determined from these measurements, since the tilting angle of the molecules contained in the unit cell does not necessarily correspond to the monoclinic angle β. The parallel packing arrangement of the neighboring molecules, which is different to the antiparallel arrangement in the bulk oligomer,[20] might be due to the particular crystallization process induced by the interaction between the molecules and the two-dimensional substrate surface.

In order to investigate the orientational distribution of the 00L reciprocal lattice for the high-T_s film, a pole figure measurement[24] was carried out where the momentum transfer q was fixed at 4.00 nm^{-1}, corresponding to the 002 reflection. A three-dimensional diagram of the intensity distribution of this reflection and its projected contour map are depicted in Figure 4. The parameters X and Y represent the two-dimensional coordinates when the scattering vector $\boldsymbol{q}_{002}$ is projected onto a virtual XY plane parallel to the surface of the substrate. The angle χ between $\boldsymbol{q}_{002}$ and the substrate normal is reduced to $(X^2 + Y^2)^{1/2}$ when $0 \le X + Y \le 90$ deg. The azimuthal angle Ψ was varied from 0 to 360 deg as $\boldsymbol{q}_{002}$ was rotated around the substrate normal. As expected, the diffraction intensity of $\boldsymbol{q}_{002}$ was confined to a narrow region around $X = Y = 0$ ($\chi = 0$), which implies that the reciprocal c^*-axis is highly oriented in the direction normal to the substrate. This also demonstrates that the *ab* lattice plane is perfectly parallel to the substrate. The fact that the lattice spacing d_{001} is smaller than the length of the oligomer molecule implies that the molecules probably tilt toward the *ab* lattice plane, supporting our conclusion that the monoclinic structure is adopted. The unit cell parameters of the high-T_s film are listed in Table 1 and compared with the corresponding values for the ferroelectric form I structure of PVDF. Although their space groups are different, the molecular

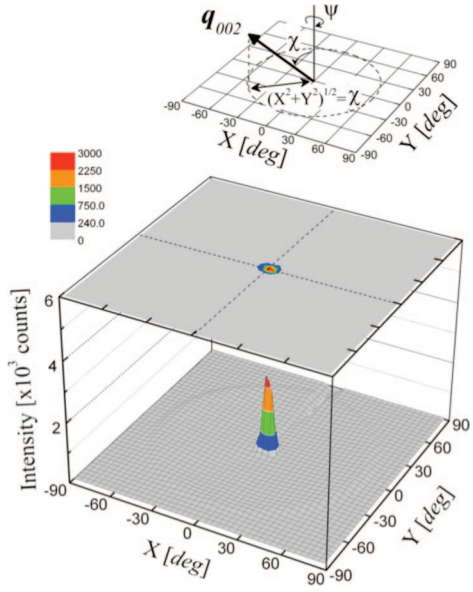

Figure 4. Pole figure profile and corresponding contour map projected onto the virtual XY plane parallel to the substrate for the high-T_s film. The momentum transfer q was fixed at 4.00 nm^{-1}, corresponding to the 002 reflection. The angle χ between the scattering vector $\boldsymbol{q}_{002}$ and the substrate normal is reduced to $(X^2 + Y^2)^{1/2}$ in the range $0 \leq X + Y \leq 90$ deg. The azimuthal rotation angle φ was varied from 0 to 360 deg.

Table 1. Structural Parameters for Ferroelectric PVDF[8] and the High-T_s VDF Oligomer (n = 12) Film

	PVDF[8]	VDF oligomer (n = 12)
crystal system	orthorhombic	monoclinic
space group	*Cm2m* (no.38)	*Cm* (no.8)
a [nm]	0.858	0.488
b [nm]	0.491	0.865
c [nm]	0.256*	3.137/sin β
β [deg]		undefined
unit cell density [g/cm^3]	1.97	2.42
	drawn and heat-treated thick film (*subcell)	thin film formed by vacuum deposition on si wafer at 310 K

packing structure in the *ab* lattice plane corresponding to the *all-trans* conformation is essentially the same in the VDF polymer and oligomer.

Finally, we probed the layer structures nondestructively by means of specular X-ray reflectivity measurements (Figure 5). The profiles of the two films are shifted for clarity by 2 orders of magnitude on the reflectivity scale. In both profiles, clear Kiessig fringes appear above the critical momentum transfer q_c of the silicon substrate. The approximate values of q_c and the film thickness were estimated by performing a simple Fourier transformation of the Kiessig fringes using the software 'MUREX'.[25] The symmetric Fourier amplitude, which indicates that the transformation is valid, is depicted in the inset of Figure 5. The position of the peak corresponds to the thickness of the oligomer film. When the q_c values were fixed at 0.29 nm^{-1} (low-T_s) and 0.30 nm^{-1} (high-T_s), the thicknesses of the films were determined as 177.4 and 143.3 nm, respectively. The average film density was also calculated using the q_c value as follows,[26]

$$q_c \approx \frac{4\pi}{\lambda}\sin\sqrt{2\delta} \qquad (1)$$

with

$$\delta = \frac{Nr_e\lambda^2}{2\pi}\rho\frac{\sum_i (Z_i + f_i')}{\sum_i A_i} \qquad (2)$$

Here, N, λ, and r_e are Avogadro's number, the X-ray wavelength and the classical electron radius, respectively. Z_i, A_i, and f_i' are the atomic number, atomic mass and the real part of the anomalous dispersion of the ith atom in the layer, respectively. The evaluated average density was 2.0 and 2.1 g/cm^3 for the low-T_s and high-T_s films, respectively.

Although the Kiessig fringes in both reflectivity profiles seem to be single-mode at first glance, the detailed layer structures are not simple. In order to prove the layer structure precisely, fitting calculation considering interface roughness σ given by error function[27−29] was carried out for both profiles. As shown in Figure 5 (solid line), the fitting calculation using a three-layer model for the VDF layer (Si/SiO_2/VDF1/VDF2/VDF3) entirely shows good coincidence with the measured reflectivity of both the low-T_s and high-T_s films, although mono- and two-layer models were partially suitable for the profiles. The obtained multilayer parameters are listed in Table 2. We note that the layer parameters of the naturally oxidized silicon (SiO_2) were already determined from preliminary measurements; d_{SiO2}= 1.97 nm, σ_{SiO2}= 0.37 nm and ρ_{SiO2} varying linearly from 2.18 to 2.33 g/cm^3. The main part of the VDF layer (VDF3) is homogeneous, with an estimated density of 2.13 g/cm^3 (high-T_s) and 1.96 g/cm^3 (low-T_s), values that agree well with the corresponding estimations from the Fourier transformation (inset of Figure 5). However, the densities of both films are considerably lower than the values calculated (2.42 g/cm^3) from the unit cell parameters. As is apparent from the AFM topography of the high-T_s film (Figure 3), the large hexagonal crystalline grains enhance the

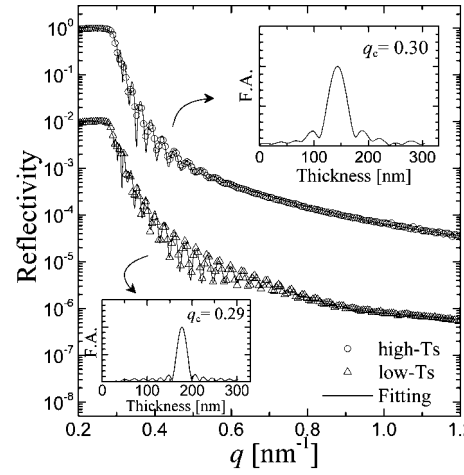

Figure 5. X-ray specular reflectivity profiles for the high-T_s film (circles), low-T_s film (triangles), and fitted reflectivity (solid line). The profiles are shifted by 2 orders of magnitude for clarity. The symmetric Fourier amplitude obtained from transformation of the Kiessig fringes is depicted in the inset. The position of the peak corresponds to the approximate thickness of the films.

Table 2. Multilayer Parameters of the Low-T_s and High-T_s Films[a]

	VDF layer	density ρ [g/cm^3]	thickness d [nm]	roughness σ [nm]
low-T_s	VDF3	1.96	167.77	3.78
	VDF2	2.12	8.18	1.40
	VDF1	1.50	1.26	0
high-T_s	VDF3	2.13	141.28	5.28
	VDF2	2.04	3.76	1.07
	VDF1	1.65	1.50	0

[a] The VDF1 and VDF3 are the bottom- and top-most layers, respectively.

surface roughness and accordingly decrease the effective film density estimated by X-ray reflectivity. In contrast, for the low-T_s film with a homogeneous, flat surface (Figure 3), the density determined by X-ray reflectivity (1.96 g/cm^3) indicates that the small crystal grains are loosely aggregated.

The VDF1 layer of considerably lower density (1.5−1.7 g/cm^3) is observed in the vicinity of the substrate surface (over the thickness of 1−2 nm) for both films. This suggests that the iodine atom bonded to the end of the oligomer molecule may not be present in the layer; the main carbon chains align perpendicular to the substrate in the first layer. Although this scenario is consistent with the structure of the high-T_s film, it appears to contradict the low-T_s structure. However, the relatively high density of the VDF2 layer in the low-T_s film (2.12 g/cm^3), which is similar to that of the VDF3 layer in the high-T_s film (2.13 g/cm^3), indicates the perpendicular molecular packing. The vertical arrangement of the VDF oligomer molecules would induce a low dielectric interface layer between the electrodes, which may cause an increase in the coercive electric field required for polarization reversal to more than 10^3 kV/cm, despite the fact that these films exhibit the highest reported remanent polarization among organic ferroelectric materials.[14,15] Rather longer VDF oligomers ($n > 12$) that exhibit a stronger interaction with the substrate may have a greater tendency to lie down on the surface, and thus might be more suitable for practical organic ferroelectric devices.

Conclusion

The unit cell, space group and layer structures of ferroelectric VDF oligomer ($n = 12$) thin films with highly oriented molecular configurations parallel (low-T_s) and perpendicular (high-T_s) to the substrate have been precisely determined using FT-IR, AFM and advanced X-ray scattering measurements. A splitting of the 130 and 200 in-plane diffraction peaks was observed for the high-T_s film, which is essential to determine the molecular packing structure. Taking into consideration the symmetry operations between the molecules, the structure could be determined as a C-centered (base-centered) monoclinic system with space group *Cm* and lattice parameters $a = 0.488$ nm, $b = 0.865$ nm, and $c = 3.137/\sin\beta$ nm. The monoclinic angle β could not be evaluated from our data. We have shown that the molecular packing arrangement in the *ab* lattice plane, based on the *all-trans* conformation, is essentially the same as that in ferroelectric PVDF. The average density evaluated from the X-ray reflectivity of both films (2.0−2.1 g/cm^3) was lower than the value calculated from the unit cell parameters (2.42 g/cm^3). This discrepancy can be explained by the surface topologies of the two films. A loose aggregate of small crystal grains is formed in the low-T_s film, while the growth of large crystalline grains in the high-T_s film results in increased surface roughness and a decrease in the effective film density. Furthermore, a density variation was observed in the vicinity of the substrate surface for both films. This suggests that the VDF molecules align vertically over a few molecular layers near the substrate surface, even in the low-T_s film where the parallel orientation is found away from the interface.

Acknowledgment. The authors thank Daikin Co., Ltd., for providing the VDF oligomer. This work was partly supported by the Grant-in-Aid for Scientific Research, the Grants for Regional Science and Technology Promotion, and the Global COE Program from the Ministry of Education, Culture, Sports, Science and Technology, by the Japan Science and Technology Agency, by Kyoto University Venture Business Laboratory, and by the Kyoto-Advanced Nanotechnology Network.

References and Notes

(1) Lando, J. B.; Olf, H. G.; Peterlin, A. *J. Polym. Sci., Part A1* **1966**, *4*, 941.
(2) Kawai, H. *Jpn. J. Appl. Phys.* **1969**, *8*, 975.
(3) Bergman, J. G.; McFee, J. H.; Crane, G. R. *Appl. Phys. Lett.* **1971**, *18*, 203.
(4) Furukawa, T.; Date, M.; Fukuda, E. *J. Appl. Phys.* **1980**, *51*, 1135.
(5) Tashiro, K.; Kobayashi, M.; Tadokoro, H.; Fukada, E. *Macromolecules* **1980**, *13*, 691.
(6) Furukawa, T.; Date, M.; Fukuda, E.; Tajitsu, Y.; Chiba, A. *Jpn. J. Appl. Phys.* **1980**, *19*, L109.
(7) Lovinger, A. J. *Science* **1983**, *220*, 1115.
(8) Hasegawa, R.; Takahashi, Y.; Chatani, Y.; Tadokoro, H. *Polym. J.* **1972**, *3*, 600.
(9) Kobayashi, M.; Tashiro, K.; Tadokoro, H. *Macromolecules* **1975**, *8*, 158.
(10) Lovinger, A. J. *Macromolecules* **1981**, *14*, 225.
(11) Lovinger, A. J. *Polymer* **1981**, *22*, 412.
(12) Yoshida, Y.; Ishida, K.; Ishizaki, K.; Horiuchi, T.; Matsushige, K. *Jpn. J. Appl. Phys.* **1997**, *36*, 7389.
(13) Noda, K.; Ishida, K.; Kubono, A.; Horiuchi, T.; Yamada, H.; Matsushige, K. *J. Appl. Phys.* **1999**, *86*, 3688.
(14) Noda, K.; Ishida, K.; Kubono, A.; Horiuchi, T.; Yamada, H.; Matsushige, K. *J. Appl. Phys.* **2003**, *93*, 2866.
(15) Horie, S.; Ishida, K.; Kuwajima, S.; Kobayashi, K.; Yamada, H.; Matsushige, K. *Jpn. J. Appl. Phys.* **2008**, *47*, 1259.
(16) Noda, K. *Doctoral Thesis*; Kyoto Univ.: Kyoto, Japan, 2002; in Japanese.
(17) Herman; Umemoto, S.; Kikutani, T.; Okui, N. *Polym. J.* **1998**, *30*, 659.
(18) Matsumoto, A.; Horie, S.; Yamada, H.; Matsushige, K.; Kuwajima, S.; Ishida, K. *Appl. Phys. Lett.* **2007**, *90*, 202906.
(19) Horie, S.; Noda, K.; Yamada, H.; Matsushige, K.; Ishida, K.; Kuwajima, S. *Appl. Phys. Lett.* **2007**, *91*, 193506.
(20) Tashiro, K.; Hanesaka, M. *Macromolecules* **2002**, *35*, 714.
(21) Doll, W. W.; Lando, J. B. *J. Macromol. Sci. Phys.* **1970**, *B2*, 889.
(22) Davis, G. T.; Mckinney, J. E.; Broadhurst, M. G.; Roth, S. C. *J. Appl. Phys.* **1978**, *49*, 4998.
(23) Takahashi, Y.; Tadokoro, H.; Odajima, A. *Macromolecules* **1980**, *13*, 1320.
(24) Bur, A. J.; Bames, J. D.; Wahlstrand, K. J. *J. Appl. Phys.* **1986**, *59*, 2345.
(25) Sakurai, K.; Iida, A. *Jpn. J. Appl. Phys.* **1992**, *31*, L113.
(26) Tolan, M. *X-ray Scattering from Soft-Matter Thin Films; Springer Tracts in Modern Physics*; Springer: Berlin, 1999; Vol. 148.
(27) Parratt, L. G. *Phys. Rev.* **1954**, *95*, 359.
(28) Névot, L.; Croce, P. *Rev. Phys. Appl.* **1980**, *15*, 761.
(29) Sinha, S. K.; Sirota, E. B.; Garof, S.; Stanley, H. B. *Phys. Rev.* **1988**, *38*, 2297.

MA802639R